Int. J. Solids Structures Vol. 19, No. 9, pp. 753–766, 1983
Printed in Great Britain.

0020–7683/83 $3.00 + .00
Pergamon Press Ltd

EVALUATION OF A UNIAXIAL, NONLINEAR, SECOND-ORDER DIFFERENTIAL OVERSTRESS MODEL FOR RATE-DEPENDENCE, CREEP AND RELAXATION

E. P. CERNOCKY†
Department of Mechanical Engineering, University of Colorado, Boulder, CO 80309, U.S.A.

and

E. KREMPL
Department of Mechanical Engineering, Aeronautical Engineering & Mechanics, Rensselaer Polytechnic Institute, Troy, NY 12181, U.S.A.

(*Received* 19 *March* 1982; *in revised form* 10 *February* 1983)

Abstract—The properties of a second-order differential equation linear in the first and second time derivatives of stress and strain but nonlinear in the overstress are investigated. The overstress is the difference between the stress and an equilibrium stress which corresponds to the limiting response in infinitely slow loading. The extension to second-order time derivatives in this nonlinear constitutive equations follows similar methods in linear viscoelasticity. The nonlinear overstress dependence of the coefficient functions is, however, maintained.

The behavior of the second-order equation is compared with that of the first-order equation. Phase-plane analysis and Poincaré-linearization are used to show that the first and second-order equations exhibit the same long time limits for constant stress(strain)-rate loading. Numerical integration involving strain(stress)-rates differing by four orders of magnitude and strain(stress)-rate jumps demonstrates that the limits are rapidly attained and that the transient behavior of the second-order equation can be different from that of the first-order equation. Strong and mild oscillatory behavior as well as monotonic behavior is possible in strain control. Stress control always results in monotonic behavior. For creep and relaxation the inelastic strain is a functional of the overstress history and the large time limit corresponds to that of the first-order equation.

Unless very strong emphasis is placed on modeling unusual transient behavior, this second-order model does not appear to be more advantageous than the first-order model.

INTRODUCTION

Experiments on metals[1–11] report significant creep and relaxation and nonlinear strain(stress)-rate dependence. To model these phenomena we have previously proposed a first-order differential constitutive equation nonlinear in the stress and strain, and linear in the stress and strain rates[12–15]. This first-order equation was reduced to the uniaxial state of stress and shown to reproduce qualitative features of experimental deformation behavior[16, 17]. The equation uses two material functions: an equilibrium stress–strain curve and a viscosity function. The inelastic strain rate is solely a function of the difference between the present stress and the equilibrium stress, and this difference is called the overstress.

This first-order equation guarantees that the stress–strain slope is unique for any specified stress, strain and strain rate[12]. Consequently two stress–strain curves corresponding to the same strain rate cannot cross each other, while experimental curves can show transient crossing (Figs. 7 and 9 of[1]). A permanent difference between two stress–strain curves pertaining to the same strain rate is reported in dynamic experiments involving strain-rate changes on some but not all metals[5–7]. This strain-rate history effect cannot be reproduced by the first-order model. The creep rate for this equation is a function of the overstress alone, but transient experimental data conflicts with this prediction (Fig. 4 of[2]). Transient experimental responses suggest that the inelastic strain rate should not depend *only* on the overstress, but steady-state experimental responses correspond to a pure overstress-dependence[1–3].

†Now at Shell Development Co., Houston, TX 77001, U.S.A.

It is known from linear viscoelasticity theory that the use of higher than first-order derivatives of stress(strain) increases the "length of the memory" and changes the transient behavior represented by the model.

Since experiments showed that the transient capabilities of the first-order model should be improved, a model was examined which contains second time derivatives of stress and strain while maintaining the nonlinear dependence on stress and strain through the overstress. The overstress dependence enabled unified modeling of rate dependence, creep and relaxation, and allowed the existence of an asymptotic solution under constant strain(stress)-rate loading at *any* value of stress and strain when the tangent modulus is small compared to the elastic modulus (the plastic range) (see [12, 16, 17]). These properties were essential in modeling the behavior of the engineering alloys tested in [1–3].

The first-order model is considered to be a valid model for metals which do not exhibit a strain-rate history effect (e.g. at least those tested in [1–3]) and as long as the overstress does not change sign [12, 15–17]. Under these conditions nonlinear viscoelasticity is indistinguishable from visco-plasticity according to the definitions given in [25]. For the representation of cyclic loading behavior of metals the first-order model, as well as the second-order model studied in this paper, must be augmented by a growth law for the equilibrium stress.

The present analysis is concerned with the qualitative properties of the second-order model under monotonic loading including creep and relaxation. No fit to experimental data is attempted. For complex constitutive equations such as this nonlinear second-order model, it is essential that qualitative properties such as asymptotic solutions, stability and transient behavior are understood before a fit to experimental data is attempted. Experience has shown that fitting a limited set of data is almost always possible with nonlinear equations with potentially disastrous results when the so-determined equation is applied to conditions different from those used in fitting the data.

THE CONSTITUTIVE EQUATION

We designate σ as the axial stress and ϵ as the infinitesimal total strain. The second order equation is

$$Eb[X]\ddot{\epsilon} + Ek[X]\dot{\epsilon} + g[\epsilon] = b[X]\ddot{\sigma} + k[X]\dot{\sigma} + \sigma. \tag{1}$$

A superimposed dot indicates differentiation with respect to time, and square brackets denote a function of the indicated argument. During loading $g[\ ]$ has the appearance of a tensile/compressive stress–strain curve, and $g[\ ]$ represents an equilibrium stress–strain response of the material. The overstress is denoted as X, where

$$X \equiv \sigma - g[\epsilon]. \tag{2}$$

The functions $b[\ ]$ and $k[\ ]$ are positive, monotonically decreasing functions of $|X|$, and E is the constant elastic modulus.

BEHAVIOR NEAR THE STRESS-STRAIN ORIGIN

To represent a region of initial elastic response we require

$$g[\epsilon] \approx E\epsilon \quad \text{for} \quad |\epsilon| < a, \tag{3}$$

where "a" is a chosen constant.

In this case the constitutive equation reduces to

$$b[X]\ddot{X} + k[X]\dot{X} + X \approx 0. \tag{4}$$

When we prescribe elastic slope *at* the origin, $X[0]$ and $\dot{X}[0]$ are zero, and (4) predicts linear elastic behavior throughout the region where (3) applies.

When $g[\ ]$ is not elastic near the origin, (3) does not apply. In this case elastic slope may still be prescribed *at* the origin, but no *region* of elastic behavior occurs (see eqn (11) below).

LIMITING STRESS-STRAIN BEHAVIOR AT LARGE TIME

The stress–strain behavior predicted by (1) at large times in strain-controlled loading is investigated by rewriting the constitutive equation as an integral equation for the overstress, assuming $X[0^-] = 0$

$$X[t] = \int_{0^-}^{t} \left((E - g')\dot{\epsilon} - \frac{b[X]}{k[X]}(\ddot{\sigma} - E\ddot{\epsilon}) \right) \exp\left(- \int_{\tau}^{t} \frac{ds}{k[X[s]]} \right) d\tau. \tag{5}$$

The distinction is made between times 0^- and 0^+ because of our subsequent use of generalized functions[18]. A prime superscript denotes differentiation of a function with respect to its argument, e.g. $g'[\epsilon] = dg/d\epsilon$.

The formal limit of (5) as time goes to infinity with the strain-rate constant provides

$$\frac{\{X\}}{k[\{X\}]} = (E - g'[\infty])\dot{\epsilon} \tag{6}$$

where braces { } denote limiting values at infinite time. Equation (6) indicates that the stress eventually grows in a manner paralleling the growth of $g[\ ]$. At large time the stress and strain continue to increase but the overstress approaches a positive bound which depends nonlinearly on the strain rate. The limit characterizes a steady-state facet of the stress–strain behavior predicted by (1) in constant strain-rate loading. Numerical solutions of (1) indicate that this limit is rapidly attained and approximately applies at small strain so that

$$\frac{X}{k[X]} \approx (E - g'[\epsilon])\dot{\epsilon}. \tag{7}$$

Because of the presence of $\ddot{\sigma}$ in the integrand of (5), execution of the limit requires the assumption that $\ddot{\sigma}[\infty]$ vanishes. Subsequent examinations of (1) in the phase plane support this assumption.

To examine the large-time (steady-state) slope of the response in constant strain-rate loading, (1) is rewritten as an integral equation for the stress rate

$$\dot{\sigma}[t] = \int_{0^-}^{t} \left(E\ddot{\epsilon} + E\frac{k[X]}{b[X]}\dot{\epsilon} - \frac{X}{b[X]} \right) \exp\left[- \int_{\tau}^{t} \frac{k}{b} ds \right] d\tau + \dot{\sigma}[0^-] \exp\left[- \int_{0^-}^{t} \frac{k}{b} ds \right]. \tag{8}$$

From the chain rule and the fact that the overstress in (6) is bounded, the limit of (8) produces

$$\left\{ \frac{d\sigma}{d\epsilon} \right\} = g'[\infty]. \tag{9}$$

Equation (9) indicates that the stress–strain responses eventually turn equidistant to each other and to $g[\ ]$ for any strain rate.

BEHAVIOR CORRESPONDING TO STRAIN-RATE JUMPS

The predictions of (1) are examined for loading with piecewise constant strain rates. At time t_0^- the strain rate is constant and equal to $\dot{\epsilon}^-$. At time t_0^+ the strain rate is instantaneously increased (decreased) to a new constant value $\dot{\epsilon}^+$. At all times other than t_0, $\ddot{\epsilon}$ is zero and for all time $\ddot{\epsilon}$ may be written as

$$\ddot{\epsilon}[t] = (\dot{\epsilon}^+ - \dot{\epsilon}^-)\delta[t - t_0] \tag{10}$$

where $\delta[\ ]$ is the Dirac delta-function. Substitution of (10) into (5) and use of (5) both before and after the strain-rate jump produces a relationship between the stress rates before and after the strain-rate jump

$$\dot{\sigma}[t_0^+] = E(\dot{\epsilon}^+ - \dot{\epsilon}^-) + \dot{\sigma}[t_0^-]. \tag{11}$$

If the slope prior to the jump is small compared with E, the term $\dot{\sigma}[t_0^-]$ is negligible in (11), and

$$\frac{d\sigma[t_0^+]}{d\epsilon} \approx E(1-\dot{\epsilon}^-/\dot{\epsilon}^+). \tag{12}$$

Table 1 summarizes the predictions corresponding to large increases and decreases in the strain rate and stress rate.

When a strain-rate jump occurs at the start of loading from the origin, $\dot{\sigma}^- = \dot{\epsilon}^- = 0$ in (11), and the initial stress–strain slope always equals E.

RESPONSES FOR THE LIMITS OF LARGE AND SMALL STRAIN-RATES

At the start of constant strain-rate loading the strain-rate jumps to a constant value denoted as γ; $\dot{\epsilon}^+ = \gamma$. Using $\epsilon = \gamma t$, the chain rule, (8) and (10), the stress–strain slope for time $t \geq 0^-$ is

$$\sigma'[\epsilon] = E + \frac{1}{\gamma}\int_{0^-}^{\epsilon}\left(E\frac{k[X]}{b[X]} - \frac{X}{b[X]\gamma}\right)\exp\left[-\frac{1}{\gamma}\int_{\hat{\epsilon}}^{\epsilon}\frac{k[X[s]]}{b[X[s]]}ds\right]d\hat{\epsilon}. \tag{13}$$

The limit of (13) as $\gamma \to \infty$ results in the slope for loading at an infinite strain-rate

$$\lim_{\substack{\gamma\to\infty \\ \epsilon \text{ finite}}} \sigma'[\epsilon] = E. \tag{14}$$

To examine loading at the limit of zero strain-rate, we differentiate $\dot{\sigma}[t]$ using (8), (10), (11), and use the theory of generalized functions[18, 19] to obtain

$$\ddot{\sigma}[t] = E(\dot{\epsilon}^+ - \dot{\epsilon}^-)\delta[t-t_0] + \ddot{\sigma}_A[t] \tag{15}$$

where $\ddot{\sigma}_A[t]$ is an analytic function. Substitution of (10) and (15) into (5) with $\epsilon = \gamma t$ yields

$$X = \int_{0^-}^{\epsilon}\left(E - g' - \frac{b[X]}{k[X]}\gamma^2\frac{d^2\sigma_A}{d\epsilon^2}\right)\exp\left[-\frac{1}{\gamma}\int_{\hat{\epsilon}}^{\epsilon}\frac{ds}{k[X[s]]}\right]d\hat{\epsilon} \tag{16}$$

Table 1. Stress–strain slopes immediately following large strain(stress)-rate increases, decreases and reversals

a) Strain-rate Changes[1)]

			Reversal		
	Increase	Decrease	-	Decrease	Increase
	$\delta >> 1$[2)]	$0 < \delta << 1$	$\delta = -1$	$1/\delta << -1$	$\delta << -1$
$\frac{d\sigma^+}{d\epsilon}$	E	$-E/\delta$	2E	$E/\lvert\delta\rvert$	E

b) Stress-rate Changes[1)]

			Reversal		
	Increase	Decrease	-	Decrease	Increase
	$\Delta >> 1$[3)]	$0 < \Delta << 1$	$\Delta = -1$	$1/\Delta << -1$	$\Delta << -1$
$\frac{d\sigma^+}{d\epsilon}$	E	$\Delta\, d\sigma/d\epsilon^-$	$-d\sigma/d\epsilon^-$	$-\lvert\Delta\rvert d\sigma/d\epsilon^-$	E

[1)] $d\sigma/d\epsilon^- << E$ is assumed

[2)] $\delta = \dot{\epsilon}^+/\dot{\epsilon}^-$ [3)] $\Delta = \dot{\sigma}^+/\dot{\sigma}^-$

and the limit of (16) as $\gamma \to 0$ furnishes

$$\lim_{\substack{\gamma \to 0 \\ \epsilon \neq 0}} \sigma[\epsilon] = g[\epsilon]. \tag{17}$$

Equation (17) is the reason that $g[\,]$ is identified as the equilibrium stress–strain curve for the material.

THE PHASE PLANE FOR CONSTANT STRAIN-RATE LOADING

The constitutive equation may be analyzed in the phase plane for constant strain-rate loading when

$$g'[\,] \approx E_t = \text{constant}$$

and (18)

$$g''[\,] \approx 0.$$

Substitution of (2) and (18) into (1) results in

$$\ddot{X} + \frac{k[X]}{b[X]}\dot{X} + F[X] = 0 \tag{19}$$

where

$$F[X] \equiv \frac{X - (E - E_t)k[X]\dot{\epsilon}}{b[X]}. \tag{20}$$

The strain rate acts as a constant parameter in (20). Equation (19) is a particular case of Lienard's equation[20], for which the phase plane approach is well established. Here the method of Liapunov[20] is used to establish asymptotic stability in the entire phase plane.

By defining $V[t]$ as the time derivative of the overstress

$$V[t] \equiv \dot{X}[t] \tag{21}$$

(19) may be written in the $X - V$ phase plane as

$$\frac{dV}{dX} = -\frac{F[X] + \dfrac{k[X]}{b[X]}V}{V}. \tag{22}$$

The only singular point of (22) is (X_0, V_0) where $V_0 = 0$ and where X_0 satisfies $F[X_0] = 0$. This condition requires

$$X_0 = (E - E_t)k[X_0]\dot{\epsilon}. \tag{23}$$

In (23) X_0 satisfies the same transcendental equation which the overstress-limit satisfies in (6). Because $k[\,]$ is a monotonically decreasing function of $|X_0|$, the value of X_0 in (23) is unique for any chosen strain rate. The solution of (1) approaches (X_0, V_0) with infinite time and the overstress approaches the limit in (6) if and only if the singular point (X_0, V_0) is stable.

To represent a Liapunov function indicating the region of stability of (X_0, V_0) we define

$$Y[t] \equiv V[t] + H[X[t]] \tag{24}$$

where

$$H[X] \equiv \int_{X_0}^{X} k[s]/b[s]\,ds. \tag{25}$$

Then a Liapunov function for this constitutive equation is[20],

$$L[X, V] \equiv \frac{1}{2}Y^2 + \int_{X_0}^{X} F[s]\,ds \tag{26}$$

and (X_0, V_0) is an *asymptotically* stable critical point of the constitutive equation if[20]

$$F[X]H[X] > 0 \tag{27}$$

$$T[X] = \int_{X_0}^{X} F[s]\,ds > 0. \tag{28}$$

Because $k[\ ]$ and $b[\ ]$ are positive functions for all overstress, the integrand of (25) is always positive. Using the integral mean value theorem[21] and the transformation $X = Z + X_0$, (25) may be written as

$$H = \int_0^Z \frac{k[\hat{Z} + X_0]}{b[\hat{Z} + X_0]}\,d\hat{Z} = \frac{k[Z_0 + X_0]}{b[Z_0 + X_0]}Z \tag{29}$$

where $Z/Z_0 > 1$. Because $b[\ ]$ and $k[\ ]$ are always positive, from (29)

$$H[Z + X_0] \gtrless 0 \quad \text{for} \quad Z \gtrless 0 \tag{30}$$

and the stability requirement (27) is satisfied if

$$F[Z + X_0] \gtrless 0 \quad \text{for} \quad Z \gtrless 0. \tag{31}$$

Using Z and the integral mean value theorem[21], (28) becomes

$$T[Z + X_0] = F[Z_1 + X_0]Z > 0 \tag{32}$$

where Z_1 is an unknown point and $Z/Z_1 > 1$. From (32) the stability requirement (28) is also satisfied if (31) is true.

From (20) and (23)

$$F[Z + X_0] = \frac{k[X_0]\,(Z + X_0) - X_0 k[Z + X_0]}{b[Z + X_0]k[X_0]}. \tag{33}$$

Using (33) and the fact that $b[\ ]$ and $k[\ ]$ are always positive, the stability condition (31) becomes

$$P[Z + X_0] \gtrless P[X_0] \quad \text{for} \quad Z \gtrless 0 \tag{34}$$

where

$$P[X] = \frac{X}{k[X]}. \tag{35}$$

Because $k[\ ]$ is a decreasing function of $|X|$, $P'[X]$ is always positive and $P[X]$ has the monotonically increasing form shown in Fig. 1. Figure 1 shows that (34) is satisfied for any critical point X_0 and any increment Z. Consequently the critical point (X_0, V_0) is asymptotically stable in the entire phase plane.

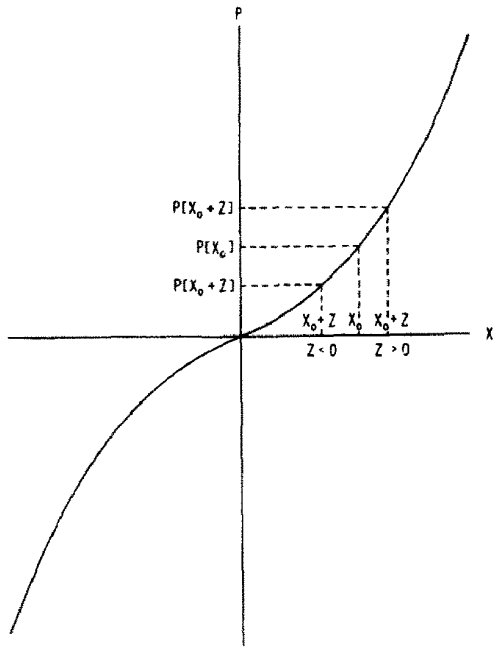

Fig. 1. Schematic depicting P vs X to show that (34) is satisfied for every Z and X_0.

During different phases of loading, the stress–strain response may be monotonic or it may oscillate, but eventually $X \to X_0$ with large time. Through appropriate selection of the functions $b[\ ]$ and $k[\ ]$, the responses can reach(X_0, V_0) rapidly and at infinitesimal strain. This is demonstrated for the numerical solutions of (1) in Figs. 2–6 corresponding to the particular functions listed in Table 2.

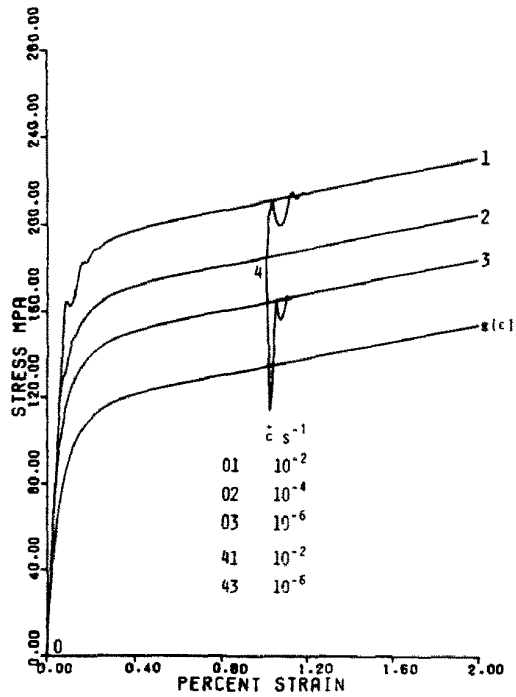

Fig. 2. Numerical experiment using piecewise constant strain rates. Damped oscillations occur at the end of the elastic region and immediately after the strain-rate jumps. $\alpha = 2$. Material functions are given in Table 2.

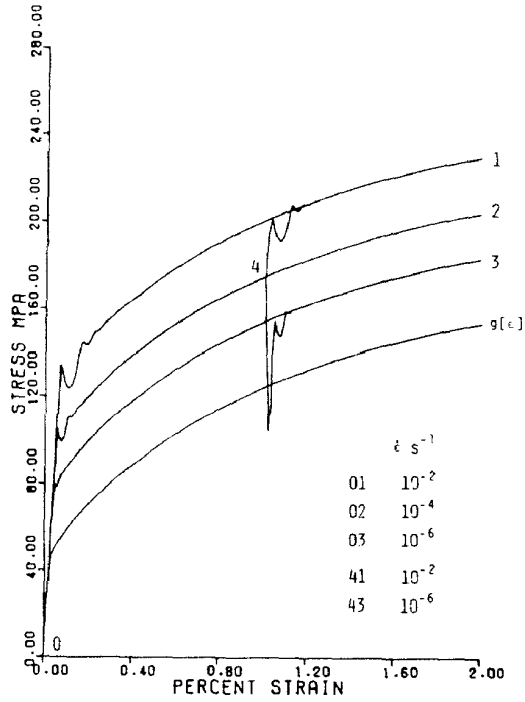

Fig. 3. Same as Fig. 2 except a g-curve with continuously decreasing slope is used from Table 2.

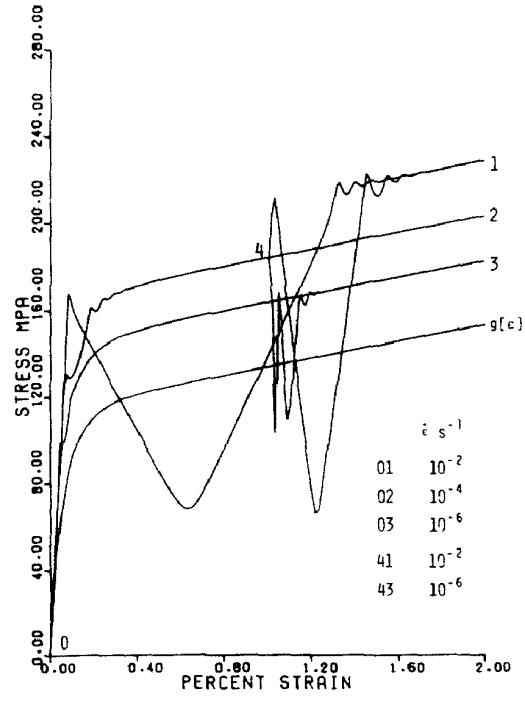

Fig. 4. Same as Fig. 2 except $\alpha = 1$, causing oscillatory behavior. Material functions from Table 2.

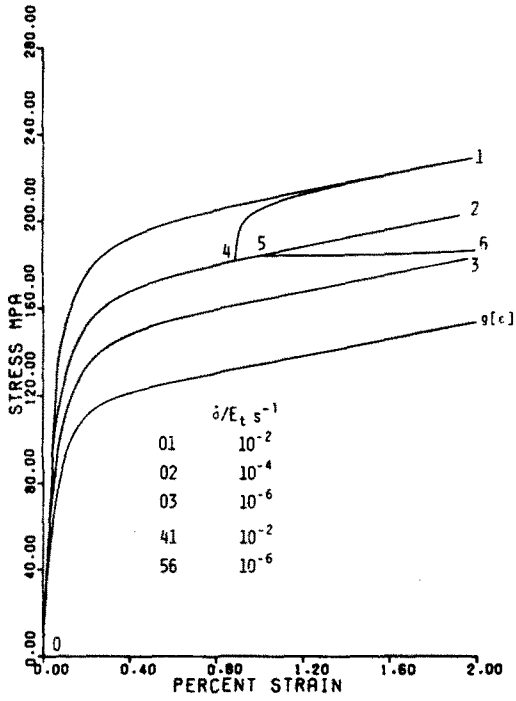

Fig. 5. Stress control with stress-rate jumps for $\alpha = 1$. Unlike Fig. 4, no oscillations occur. Same material functions as in Fig. 4.

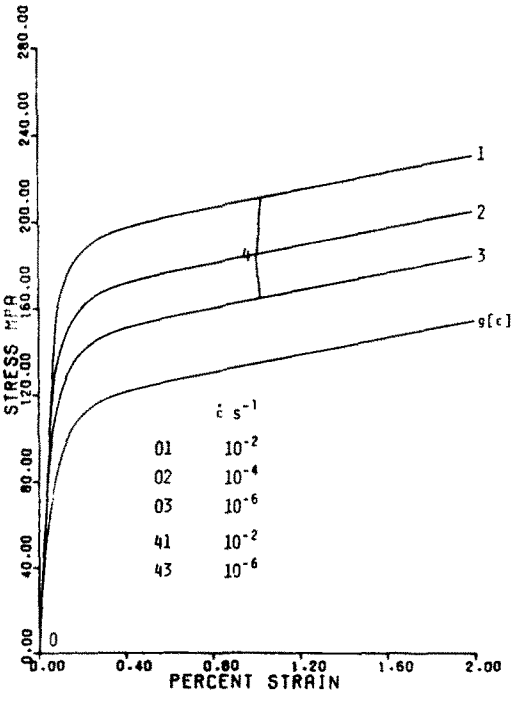

Fig. 6. Same as Fig. 2 except $\alpha = 60$. No oscillations occur, the singular point is a node, and the responses match the responses of the first-order equation.

THE PHASE PLANE FOR CONSTANT STRESS-RATE LOADING

The phase plane is examined in constant stress-rate loading when (18) applies. From (2) and (18)

$$\dot{\epsilon} = -(\dot{X} - \dot{\sigma})/E_t \tag{36}$$

and

$$\ddot{\epsilon} = -\ddot{X}/E_t \tag{37}$$

where $E_t > 0$. Substitution of (36), (37) and (2) into (1) furnishes

$$\ddot{X} + \frac{k[X]}{b[X]}\dot{X} + U[X] = 0 \tag{38}$$

where

$$U[X] = \frac{E_t X - (E - E_t)k[X]\dot{\sigma}}{Eb[X]}. \tag{39}$$

In stress control the singular point is (X_0, V_0) where $V_0 = 0$ and where X_0 satisfies $U[X_0] = 0$. From (39) this requires

$$X_0 = (E - E_t)k[X_0]\dot{\sigma}/E_t. \tag{40}$$

Because of the slope limit in (9), the values of X_0 are the same in (23) and (40), and (1) predicts the same limiting overstress in stress and strain control. Comparison of (38)–(40) with (19)–(23) indicates that the proof of stability of (X_0, V_0) is the same for stress and strain control. Consequently when (18) applies, all solutions in constant stress-rate loading approach the limiting overstress X_0 in (40). Again $X \approx X_0$ at small strain for our particular choice of material functions (Fig. 5).

Table 2. Material functions used

Figures 2 - 6

$$k[X] = A(1 + |X|/B)^{-m}$$

$A = 314200$ s $B = 71.38$ MPa $m = 21.98$

Figures 2, 4 - 6

$$g[\epsilon] = E_t\epsilon + \frac{E - E_t}{C}\left(4(U - V) + (1 + U)^{-4} - (1 + V)^{-4}\right)$$

$C = 45.3$ $E = 194.8$ GPa $E_t = 1.934$ GPa

$U = |.00338 + 338\,\epsilon|$ $V = |.00338 - 338\,\epsilon|$

Figure 3

$$g[\epsilon] = \begin{cases} E\epsilon & \epsilon \le \epsilon_o \\ E\epsilon - D(\epsilon - \epsilon_o)^{1.02} & \epsilon \ge \epsilon_o \end{cases}$$

$\epsilon_o = .00023$ $E = 194.8$ GPa $D = 204.73$ GPa

Integration was performed using the algorithm of [24].

CREEP BEHAVIOR

For a constant-stress creep test started at time t_0 we rewrite (1) as an integral equation for the creep rate for $t \geq t_0$

$$\dot{\epsilon}_c[t] = \dot{\epsilon}_{in}[t_0^-] \exp\left[-\int_{t_0}^{t} \frac{k[X[s]]}{b[X[s]]} ds\right] + \int_{t_0}^{t} \frac{X}{Eb[X]} \exp\left[-\int_{\tau}^{t} \frac{k[X[s]]}{b[X[s]]} ds\right] d\tau \tag{41}$$

where $\dot{\epsilon}_{in}[t]$ denotes the inelastic strain rate defined by

$$\dot{\epsilon}_{in}[t] \equiv \dot{\epsilon}[t] - \dot{\sigma}[t]/E. \tag{42}$$

From the formal limit of (41) we obtain the limit of the creep rate as $t \to \infty$

$$\{\dot{\epsilon}_c\} = \frac{\{X\}}{Ek[\{X\}]} \tag{43}$$

where

$$\{X\} = \sigma_0 - g[\{\epsilon\}] \tag{44}$$

and σ_0 is the constant stress in the test.

The phase-plane analysis in stress control applies to the creep test provided (18) applies with $E_t > 0$. From (40) $X_0 = 0$ in this case, and creep terminates at a total strain

$$\{\epsilon\} = g^{-1}[\sigma_0]. \tag{45}$$

However if $E_t \leq 0$ the phase plane analysis does not apply, and the creep rate becomes constant or increases. Then secondary and tertiary creep are reproduced by (1), see also (43) and (44).

RELAXATION BEHAVIOR

For a constant-strain relaxation test started at time t_0, substitution of (10) into (8) provides, for $t \geq t_0$

$$\dot{\sigma}[t] = -E\dot{\epsilon}_{in}[t_0^-] \exp\left[-\int_{t_0}^{t} \frac{k[X[s]]}{b[X[s]]} ds\right] - \int_{t_0}^{t} \frac{X}{b[X]} \exp\left[-\int_{\tau}^{t} \frac{k[X[s]]}{b[X[s]]} ds\right] d\tau. \tag{46}$$

From the formal limit of (46) we obtain the limit of the relaxation rate as $t \to \infty$

$$\{\dot{\sigma}\} = -\frac{\{X\}}{k[\{X\}]} \tag{47}$$

where

$$\{X\} = \{\sigma\} - g[\epsilon_0] \tag{48}$$

and ϵ_0 is the constant strain in the relaxation test.

In a relaxation test the phase plane analysis for strain control applies without requiring (18); (19) is valid for all strain. In relaxation $X_0 = 0$ and relaxation terminates at an equilibrium stress given by

$$\{\sigma\} = g[\epsilon_0]. \tag{49}$$

FORMULATION IN TERMS OF THE INELASTIC STRAIN RATE

Equation (1) can be rewritten in terms of the inelastic strain rate defined in (42) to obtain

$$\ddot{\epsilon}_{in} + \frac{k[X]}{b[X]}\dot{\epsilon}_{in} = \frac{X}{Eb[X]}, \tag{50}$$

which can be transformed into

$$\dot{\epsilon}_{in} = \dot{\epsilon}_{in}[t_0^-] \exp\left[-\int_{t_0}^{t} \frac{k[X[s]]}{b[X[s]]}\,ds\right] + \int_{t_0}^{t} \frac{X}{Eb[X]} \exp\left[-\int_{\tau}^{t} \frac{k[X[s]]}{b[X[s]]}\,ds\right] d\tau. \tag{51}$$

Equation (51) has an asymptotic limit for $t \to \infty$,

$$\{\dot{\epsilon}_{in}\} = \frac{\{X\}}{Ek[\{X\}]}. \tag{52}$$

With the assumptions of $\dot{\epsilon}_{in}[t_0^-] = 0$ and $t_0 = 0$ and using (42), eqn (51) furnishes

$$\dot{\epsilon} = \dot{\sigma}/E + \int_{0}^{t} \frac{X}{Eb[X]} \exp\left[-\int_{\tau}^{t} \frac{k[X[s]]}{b[X[s]]}\,ds\right] d\tau. \tag{53}$$

Equation (51) shows that the inelastic strain rate is continuous even if the stress and total strain rates are discontinuous. Equation (53) shows that the inelastic strain rate is a functional of the overstress history.

From (53) for initially positive (negative) overstress the inelastic strain rate is always positive (negative), and from (42) and (53) the strain rate is always positive (negative) for stress control with a positive (negative) stress rate. Consequently the stress–strain slope is positive and the stress can never oscillate in stress control.

DISCUSSION

The stress–strain slopes predicted after strain(stress)-rate jumps, the responses near the origin, and the limiting responses in constant stress(strain)-rate loading are identical for the first- and second-order models[12]. Equations (43) and (47) show that the respective creep and relaxation responses of the second-order theory eventually coincide with the responses of the first-order theory. In relaxation the phase plane analysis applies independent of $g'[\ ]$, but in creep both (45) and the phase plane analysis apply only when $g' = E_t > 0$. Equilibrium in creep is never attained when $E_t \leq 0$, and this case corresponds to secondary and tertiary creep. The case $E_t > 0$ corresponds to primary creep only.

However the transient responses of (1) can be very different from those of the first-order equation. Poincaré-linearization of (22) in the phase plane[23] shows that (X_0, V_0) is either a stable node or a stable spiral in strain control.† The transition from spiral to node occurs when

$$b_0 = \frac{k_0^2}{\alpha_T} \tag{54}$$

where

$$\alpha_T = 4\left(1 - X_0 \frac{k_0'}{k_0}\right) \tag{55}$$

and where $k_0 = k[X_0]$, $k_0' = (dk/dX)|_{X_0}$, and $b_0 = b[X_0]$. When the r.h.s. of (54) is greater (smaller) than b_0, the singular point is a node (spiral). For the particular k-function of Table 2, α_T is bounded by $4 \leq \alpha_T \leq 91.92$.

Because of the local stability relationship (54) and because of dimensional similitude, we use the relationship

$$b[X] = \frac{k^2[X]}{\alpha} \tag{56}$$

to demonstrate particular numerical solutions of (1). From (54) to (56) the stress–strain responses should correspond to a spiral singularity for $\alpha < \alpha_T$, and a nodal singularity for

†For stress control and $E_t > 0$ the singular point is always a stable node.

$\alpha > \alpha_T$ in (56). Because X_0 is rate dependent through (23), α_T is rate dependent and changes with the limiting overstress X_0.

The numerical solution of (1) in Fig. 2 corresponds to the material functions in Table 2, with $\alpha = 2$. From (55) $\alpha_T > 4$, and consequently the Poincaré-linearization predicts that each limit for the responses in Fig. 2 is a spiral singularity. The stress–strain responses oscillate during the transient stress–strain behavior at the knees of the stress–strain curves and after the strain-rate jumps. The singular points (limiting overstresses) are rapidly attained, and the limits in (7) apply at very small strain.

Figure 3 demonstrates that the limits can also apply for $g' \neq$ constant. The stress–strain behavior of Fig. 3 parallels the behavior in Fig. 2 although the g-function in Fig. 3 has a continually changing slope.

Figure 4 corresponds to $\alpha = 1 \ll \alpha_T$, and this produces even stronger oscillations in the stress–strain behavior about the spiral singularity than shown in Fig. 2. Despite these oscillations, the limits are still attained within infinitesimal strain.

Stress control is simulated in Fig. 5, using the same functions and the same value of α as in Fig. 4. No oscillations occur and this corresponds to the prediction of (53).

Figure 6 shows strain-controlled responses for $\alpha = 60$, and this α-value exceeds the α_T for the highest strain rate used in the figure. The Poincaré-linearization predicts a nodal singularity, and indeed no oscillations occur. The singularity is a node and the stress–strain responses match the responses of the first-order model (see [12]).

The analysis shows that the behavior of the second-order equation is much more complicated than that of the first-order equation. Their transient behaviors differ substantially but both exhibit the same long-term behavior (see (6), (9), (43), (47) and (52)). Both models exhibit continuity of the inelastic strain rate upon discontinuities of the stress or strain rate. The second-order model therefore includes the properties of the first-order model for long-term behavior and adds capabilities for the transient responses.

The transient behavior of the second-order model can be very undesirable as Fig. 4 indicates.‡ The phase-plane analysis permits the identification of the regions where the oscillations occur by means of (55). A comparison of Figs. 4 and 6 shows that both strongly oscillatory behavior and nonoscillation can be obtained.

The strain-rate dependence of α_T in (55) indicates that for a particular α the behavior can range from oscillatory to nonoscillatory at different strain rates. Such behavior was found in unpublished experiments.

Once $b[X]$ and $k[X]$ are chosen to fit stress–strain curves, the creep and relaxation behavior are determined (see (41) and (46)).

For convenience the numerical experiments were restricted to $k^2[X]/b[X] =$ constant, and $k[X]$ was chosen to give the spacing of the stress–strain curves obtained at various strain rates shown in the figures. Further analysis could be performed where $k^2[X]/b[X] =$ a suitable function. Numerical experiments will be necessary to ascertain the behavior under these conditions.

When mildly-oscillatory or nonoscillatory behavior is observed, the transition to steady-state behavior is very quick (see Figs. 2, 3 and 6). It was not possible to obtain a gradual transition even by increasing α well beyond α_T; this second-order model cannot represent the strain-rate history effect.

The model proposed in (1) permits additional flexibilities by not requiring that the ratio of the coefficient functions of $\dot{\epsilon}$ and $\dot{\sigma}$ are equal to E. Preliminary numerical experiments indicate that it is then possible to obtain a very gradual transition modeling a strain-rate history effect [5–7]. This additional possibility needs to be explored in a systematic fashion.

The numerical integration of (1) requires much more CPU time than the first-order equation. Although the CPU time depends strongly on the parameters chosen, it is typically three to four times longer than for the first-order equation.

CONCLUSION

The second-order equation enhances the transient capabilities of the first-order equation

‡Irregularities such as the Portevin le Chatelier effect are usually of small amplitude at room temperature: at high temperature large transient oscillations reaching the zero axis have been reported.

considerably. The long-term limits are, however, identical for both equations. Unless very strong requirements are imposed on the modeling of oscillatory transient behavior, the use of the second-order model in solving boundary value problems is not recommended.

Acknowledgement—This research was supported by the National Science Foundation. Early discussions with A. Meyer contributed to the solution methods.

REFERENCES

1. E. Krempl, An experimental study of room-temperature rate-sensitivity creep and relaxation of AISI type 304 stainless steel. *J. Mech. Phys. Solids* **27**, 363–375 (1979).
2. D. Kujawski, V. Kallianpur and E. Krempl, An experimental study of uniaxial creep, cyclic creep and relaxation of AISI type 304 stainless steel at room temperature. *J. Mech. Phys. Solids* **28**, 129–148 (1980).
3. D. Kujawski and E. Krempl, The rate (time)-dependent behavior of the Ti-7Al-2Cb-1Ta titanium alloy at room temperature under monotonic and cyclic loading. *Trans. ASME, J. Appl. Mech.* **48**, 55–63 (1981).
4. C. Albertini and M. Montagnani, Wave propagation effects in dynamic loading. *Nucl. Engng Design* **37**, 115–124 (1976).
5. B. Dodd, R. C. Stone and J. D. Campbell, The strain-rate sensitivity of 304L austenitic stainless steel in uniaxial tension. Oxford University, *Rep. No.* 1069/73 (1973).
6. R. A. Frantz Jr. and J. Duffy, The dynamic stress–strain behavior in torsion of 1100-0 aluminum subjected to a sharp increase in strain rate. *Trans. ASME, J. Appl. Mech.* **39**, 939–945 (1972).
7. T. Nicholas, Strain-rate and strain-rate-history effects in several metals in torsion. *Exper. Mech.* **11**, 370–374 (1971).
8. C. J. Maiden and S. J. Green, Compressive strain-rate tests on six selected materials at strain rates from 10^{-3} to 10^{4} sec^{-1}. *Trans. ASME, J. Appl. Mech.* **33**, 496–504 (1966).
9. C. H. Karnes and E. A. Ripperger, Strain rate effects in cold worked high-purity aluminum. *J. Mech. Phys. Solids* **14**, 75–88 (1966).
10. J. R. Ellis, D. N. Robinson and C. E. Pugh, Behavior of annealed type 316 stainless steel under monotonic and cyclic biaxial loading at room temperature. *Nucl. Engng Design* **47**, 115–123 (1978).
11. J. F. Thomas Jr. and F. L. Yaggee, Stress relaxation in solution-annealed and 20 percent cold-worked type 316 stainless steel. *Met. Trans.* **6A**, 1835–1837 (1975).
12. E. P. Cernocky and E. Krempl, A nonlinear uniaxial integral constitutive equation incorporating rate effects, creep and relaxation. *Int. J. Non-Linear Mech.* **14**, 183–203 (1979).
13. E. P. Cernocky and E. Krempl, A theory of thermoviscoplasticity for uniaxial mechanical and thermal loading. *J. Mécanique Appliquée* **5**, 293–321 (1981).
14. E. P. Cernocky and E. Krempl, A theory of thermoviscoplasticity based on infinitesimal total strain. *Int. J. Solids Structures* **16**, 723–741 (1980).
15. E. P. Cernocky and E. Krempl, A theory of viscoplasticity based on infinitesimal total strain. *Acta Mechanica* **36**, 263–289 (1980).
16. M. C. M. and E. Krempl, A uniaxial viscoplastic model based on total strain and overstress. *J. Mech. Phys. Solids* **27**, 377–391 (1979).
17. E. Krempl, The role of servocontrolled testing in the development of the theory of viscoplasticity based on total strain and overstress. *ASTM STP* 765, pp. 5–28, American Society for Testing and Materials (March 1982).
18. G. Doetsch, *Introduction to the Theory and Application of the Laplace Transformation*. Springer Verlag, Berlin (1974).
19. A. N. Kolmogorov and S. V. Fomin, *Introductory Real Analysis*. Prentice Hall, Englewood Cliffs, New Jersey (1970).
20. R. A. Struble, *Nonlinear Differential Equations*. McGraw-Hill, New York (1962).
21. R. G. Bartle, *The Elements of Real Analysis*, 2nd Edn. Wiley, New York (1975).
22. E. P. Cernocky and E. Krempl, A coupled theory of thermoviscoplasticity based on total strain and overstress and its predictions in monotonic torsional loading. *J. Thermal Stresses* **4**, 69–82 (1981).
23. W. E. Boyce and R. C. DiPrima, *Elementary Differential Equations and Boundary Value Problems*, 3rd Edn. Wiley, New York (1977).
24. R. Bulirsch and J. Stoer, Numerical treatment of ordinary differential equations by extrapolation methods. *Numerische Mathematik* **8**, 1–13 (1966).
25. E. Krempl, Plasticity and variable heredity. *Archives of Mechanics* **33**, 289–306 (1981).